chemosensors

Article

Enzyme Inhibition-Mediated Distance-Based Paper Biosensor for Organophosphate Pesticide Detection in Food Samples

Yulin Liu [1,2,†], Longzhan Dong [2,†], Qiognzheng Hu [1,*], Jingbo Chen [2] and Mashooq Khan [1,*]

[1] Shandong Analysis and Test Center, Qilu University of Technology (Shandong Academy of Sciences), Jinan 250014, China; xiaohang880605@163.com
[2] Department of General Surgery, The First Affiliated Hospital of Shandong First Medical University, Jinan 250014, China; donglongzhan@163.com (L.D.); qychenjingbo@163.com (J.C.)
* Correspondence: huqz@qlu.edu.cn (Q.H.); khan1985@qlu.edu.cn (M.K.)
† These authors contributed equally to this work.

Abstract: Organophosphate pesticides (OPs) enter the environment through various avenues, posing significant health risks. This highlights the need to monitor OPs in food and environmental samples. This study introduces an enzyme inhibition-mediated distance-based paper (EIDP) biosensor designed for naked-eye visual detection of OPs in food samples. We synthesized a copper alginate (Cu-Alg) hydrogel that traps water within the gel and restricts water flow on pH paper. When incubated with acetylcholinesterase (AChE) and acetylthiocholine (ATCh), the enzyme activity of AChE on ATCh generates thiocholine, which interacts with the Cu^{2+} ions in the gel. This interaction alters the gel's 3D structure, releasing the trapped water onto the pH paper. Conversely, when AChE is exposed to OPs, its activity is inhibited, limiting the water flow from the gel. As a result, OPs are quantified by measuring the reduction in water flow distance within a linear range of 18 to 105 ng/mL, with a lower detection limit of 18 ng/mL. The EIDP biosensor exhibits high selectivity for OP detection and successfully analyzes OPs in pumpkin and rice samples, achieving percent recoveries ranging from 93% to 103%. This method offers a straightforward, portable, instrument-free, and cost-effective solution for detecting OPs in food samples.

Keywords: paper biosensor; enzyme inhibition; label free; instrument free; malathion

check for updates

Received: 13 March 2025
Revised: 14 April 2025
Accepted: 15 April 2025
Published: 16 April 2025

Citation: Liu, Y.; Dong, L.; Hu, Q.; Chen, J.; Khan, M. Enzyme Inhibition-Mediated Distance-Based Paper Biosensor for Organophosphate Pesticide Detection in Food Samples. *Chemosensors* **2025**, *13*, 147. https://doi.org/10.3390/chemosensors13040147

Copyright: © 2025 by the authors. Licensee MDPI, Basel, Switzerland. This article is an open access article distributed under the terms and conditions of the Creative Commons Attribution (CC BY) license (https://creativecommons.org/licenses/by/4.0/).

1. Introduction

Organophosphorus pesticides (OPs) are extensively employed in agriculture worldwide to safeguard crops from harmful insects and mites. Compared to organochlorine insecticides, such as dichlorodiphenyltrichloroethane (DDT), aldrin, and lindane, OP compounds are favored due to their greater efficacy against most insects and their cost-effectiveness; they enhance crop yield and quality [1]. Unfortunately, OPs can enter the environment through various means, including agricultural runoff, improper disposal, and accidental spills during application or transportation [2]. These compounds can persist in soil and water, negatively affecting the targeted pests and non-target organisms, wildlife, and ultimately human populations through contaminated food and water sources. The health risks associated with OPs are considerable, particularly because they work by inhibiting the enzyme AChE [3]. This inhibition results in an accumulation of acetylcholine in the nervous system, leading to a range of acute and chronic symptoms, such as headaches, dizziness, respiratory distress, nausea, and, in severe cases, significant neurological damage or even death at high exposure levels [4]. Long-term exposure has also been linked to

developmental issues in children, an increased risk of cancer, and possible adverse effects on reproductive health [5]. Given the serious risks OPs present to human health and the environment, there is a pressing need to develop accurate, sensitive, and convenient methods for detecting these compounds.

Both conventional techniques and modern biosensor technologies have been employed to monitor OPs in environmental samples [6]. Conventional methods, including high-performance liquid chromatography (HPLC), gas chromatography–mass spectrometry (GC-MS), and enzyme-linked immunosorbent assays (ELISAs), are recognized for their high detection efficiency and their capability to differentiate between certain classes of OPs [7–9]. However, these methods often involve complex experimental procedures, require expensive equipment, rely on skilled technicians, and require significant time investment, making them less suitable for on-field detection and resource-limited environments. To overcome these limitations, researchers have designed a variety of sensing platforms, such as electrochemical [10,11], photoelectrochemical, and optical sensing techniques [12–14]. The optical methods encompass photoluminescence [15], chemiluminescence [16], colorimetry [17], and fluorescence [18]. These techniques primarily utilize responsive materials, including gold nanoparticles, quantum dots, polymer-dispersed metal nanoparticles, and pH-sensitive organic dyes in solution [19,20]. These serve as transducers in conjunction with enzyme activity and inhibition. Colorimetry is one method that allows instrument-free detection by the naked eye. However, it still relies on software assistance to analyze color intensity with analyte concentrations.

Distance-based biosensors provide a straightforward, instrument-free approach to visually measure the concentration of analytes. These biosensors detect variations in parameters such as length, diameter, height, or volume expansion in response to the analyte, eliminating the need for external cameras or scanners. Changes in any of these distance parameters can be directly correlated with the concentration of the analyte [21]. Additionally, the distance-based biosensor's sensitivity, specificity, and stability can be optimized by carefully selecting substrates and tailoring specific reagents [22,23].

Distance-based biosensors utilizing paper substrates are cost-effective, portable, and user-friendly tools for various analytical applications. These devices present a compelling alternative to traditional laboratory methods. For example, a distance-based biosensor was designed to detect thrombin and its inhibitors [24]. In the presence of thrombin, water flow is inhibited on the paper strip. Conversely, thrombin's activity is suppressed when an inhibitor is present, allowing water to flow through the substrate. This biosensor exhibits a linear detection range of 16 to 85 mU/mL, with a limit of detection set at 16.1 mU/mL for thrombin. Furthermore, these biosensors have been employed to analyze a variety of analytes, including carcinoembryonic antigen [25], alkaline phosphatase [26], glutathione [27], nucleic acids [28], small molecules [29], and metal ions [30]. The simplicity of their fabrication, ease of use, and potential for on-field analysis make this approach potentially transformative for food testing in resource-limited settings where access to advanced laboratory infrastructure may be restricted.

This study presents the development of an EIDP biosensor to detect OPs in food samples, utilizing malathion as a model compound. Malathion is widely used in agriculture and public health for pest control. While it is effective against various pests, its toxicity raises concerns. Malathion can affect the nervous system by inhibiting the enzyme AChE, potentially poisoning humans and wildlife. Environmental impact includes risks to non-target organisms, including beneficial insects and aquatic life, particularly when they enter waterways. Regulatory limits for malathion residues in food products vary by country; for instance, the U.S. Environmental Protection Agency (EPA) has set tolerance levels to ensure safe consumption, typically allowing residues at or below 100 to 2000 ng/mL depending on

the food item. Thus, a copper alginate (Cu-Alg) hydrogel was synthesized and evaluated for its reactivity with AChE during the hydrolysis of ATCh. This reaction resulted in the movement of trapped water within the hydrogel to flow on pH paper mounted on a polyvinyl chloride (PVC) board (Figure 1). In the presence of OPs, the activity of AChE was inhibited, reducing the water flow distance on the pH paper. The concentration of OPs in both the solution and food samples was determined by measuring the flow distance of water on the pH paper. Thus, the EIDP biosensor offers a simple, portable approach for detecting OPs in food samples.

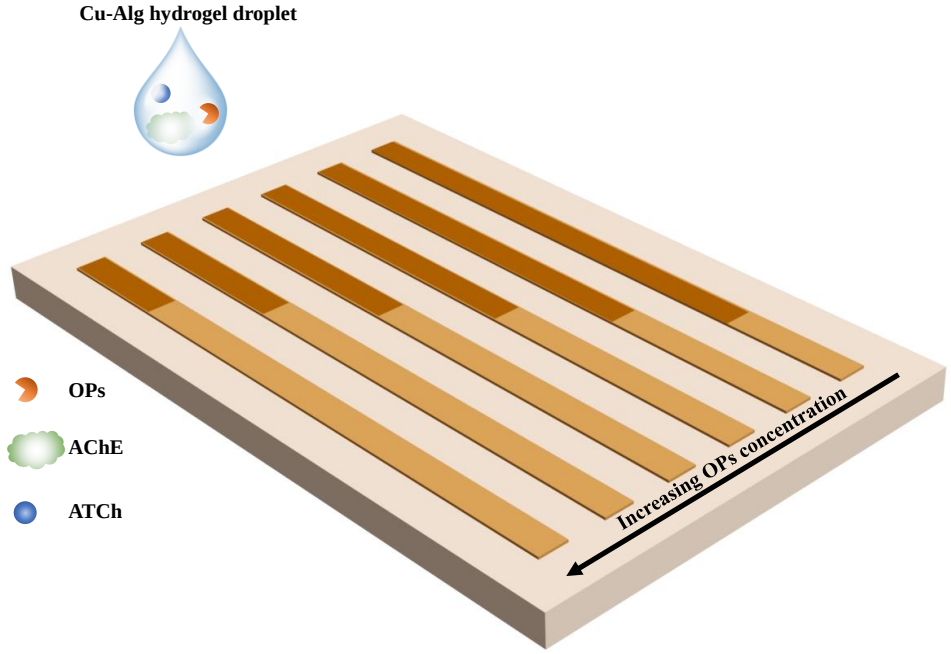

Figure 1. Schematic illustration of pH papers mounted on PVC board to construct EIDP biosensor for OP detection. OPs: organophosphate pesticides, AChE: acetylcholine esterase, ATCh: acetylthiocholine iodide.

2. Materials and Methods

2.1. Materials

ATCh and AChE were obtained from Yuanye Biotechnology Co., Ltd., Shanghai, China. Sodium alginate, cupric chloride ($CuCl_2$), glucose, fructose, 2-Pyridinealdoxime methochloride (2-PAM), and Tris(hydroxymethyl)aminomethane (Tris-HCl) were purchased from Aladdin Chemical Reagent Co., Ltd., Shanghai, China. Malathion was bought from AccuStandard Inc. (New Haven, CT, USA). All the chemicals were used without further purification. The pH papers were purchased from SSS Reagent Co., Ltd., Shanghai China. Ultrapure water was used in all experiments with a resistivity of 18.25 MΩ·cm.

2.2. Construction of EIDP Biosensor

The pH papers were cut to dimensions of 60 mm × 5 mm (length × width) and affixed to a PVC board measuring 100 mm × 75 mm × 2 mm (length × width × thickness). Before use, the papers were cleaned with ethanol and dried under nitrogen gas flow. The utilization of pH paper is preferred due to its widespread availability and application globally. No modifications were made to the paper itself. Therefore, using other porous chromatographic paper can also achieve similar results.

The Cu-Alg hydrogel was prepared by mixing sodium alginate (0.2 wt%) with varying concentrations of Cu^{2+}, namely 0.5, 1.0, 1.5, 2.0, and 2.5 mM, at room temperature. The gel's properties were evaluated by placing it on the pH paper, measuring the distance

it flowed, and conducting viscosity measurements. Furthermore, the Cu-Alg hydrogel's morphology was analyzed using scanning electron microscopy (GeminiSEM 360, ZEISS, Jena, Germany).

To analyze the feasibility of the EIDP biosensor for OP detection, the Cu-Alg hydrogel was incubated with AChE at a concentration of 0.06 U/mL and ATCh at 3 mM for 10 min. After this incubation, the hydrogel was placed on pH paper to measure its flow distance. AChE was first incubated in a separate experiment with 200 ng/mL of OPs before being combined with the Cu-Alg hydrogel and ATCh. Then, it was dropped on the pH paper for measurement. Lastly, the flow distance of the Cu-Alg hydrogel incubated with ATCh was also assessed.

2.3. Optimization Reagent Concentration and Incubation Time

Several experimental steps were undertaken to optimize various parameters, including AChE and ATCh concentrations and the incubation time of AChE with ATCh and OPs. Different AChE concentrations (0 to 0.06 U/mL) were incubated with 3 mM of ATCh and Cu-Alg for 10 min. Samples were then placed on pH paper to analyze the water's flow distance.

Subsequently, the optimal concentration of AChE in Cu-Alg was evaluated by incubating it with varying concentrations of ATCh (from 0 mM to 3 mM) for 10 min, after which aliquots were again placed on pH paper to measure the flow distance.

Furthermore, the incubation time for AChE and ATCh varied from 0 to 11 min. Finally, AChE was incubated with OPs for 0 to 30 min before incubation with ATCh and Cu-Alg.

2.4. Sensitivity and Selectivity of EIDP Biosensor

To assess the sensitivity of the EIDP biosensor, varying concentrations of OPs, ranging from 18 ng/mL to 105 ng/mL, were incubated with an AChE solution (0.05 U/mL) in a Tris-HCl buffer (20 mM, pH 7.3) at 37 °C for 30 min. The mixtures were then incubated with ATCh (2.5 mM) and the Cu-Alg hydrogel for 10 min. Finally, aliquots of the mixtures were transferred onto pH papers to quantify the distance the water migrated from the hydrogel.

The selectivity of the EIDP biosensor for detecting OPs was assessed by incubating the AChE solution separately with glucose, fructose, 2-AMP, K^+, Mg^{2+}, Ca^{2+}, glycine, L-arginine, L-cysteine, catalase, and α-amylase. Each molecule was used at a concentration of 100 μg/L. Subsequently, all the mixtures were incubated with ATCh and the Cu-Alg hydrogel. The aliquots were then placed on pH paper to evaluate the flow distance.

2.5. Analysis of Food Samples

The EIDP biosensor was employed to analyze OPs in pumpkin and rice samples. Samples of pumpkin and rice extract were prepared by crushing 1.2 g of the edible parts of a pumpkin and grinding 1.2 g of rice, which were then separately added to 4.8 mL of water. After stirring and subjecting the mixture to ultrasonic treatment for 60 min, the homogenate was centrifuged for 30 min at a speed of $3000\times g$. The supernatant was then filtered through a 0.22 μm filter membrane, and the resulting pumpkin and rice extract was collected for analysis. The extract samples were spiked with OPs to achieve 20, 50, and 100 ng/mL concentrations. The spiked samples were incubated with AChE (0.05 U/mL) for 30 min. Following this incubation, the mixture was combined with ATCh and the Cu-Alg hydrogel and incubated for 10 min. The resulting solution was then applied to pH papers to assess the flow distance. The recovery percentages and standard deviations were subsequently calculated.

3. Results

3.1. The Water Flow Distance as a Function of Cu-Alg Hydrogel Formation

We investigated the water flow distance on pH paper by dropping sodium alginate and Cu^{2+} mixture with various Cu^{2+} concentrations (0–2.5 mM). The inherent porous structure of the paper facilitates water transport through capillary action. The flow distance on the pH paper decreases significantly with an increase in Cu^{2+} concentration (Figure 2a) because the sodium ions in the alginate are replaced by Cu^{2+} ions, resulting in the formation of Cu-Alg hydrogels. When the Cu^{2+} concentration exceeds 2 mM, water becomes entirely trapped within the hydrogel, preventing it from flowing on the pH paper. To better quantify the flow distance of the solution on the pH paper, we calculated the water coverage ratio (Cr) in percent, which is the distance that water travels from the Cu-Alg hydrogel on the pH paper, with the corresponding values presented in Figure 2b.

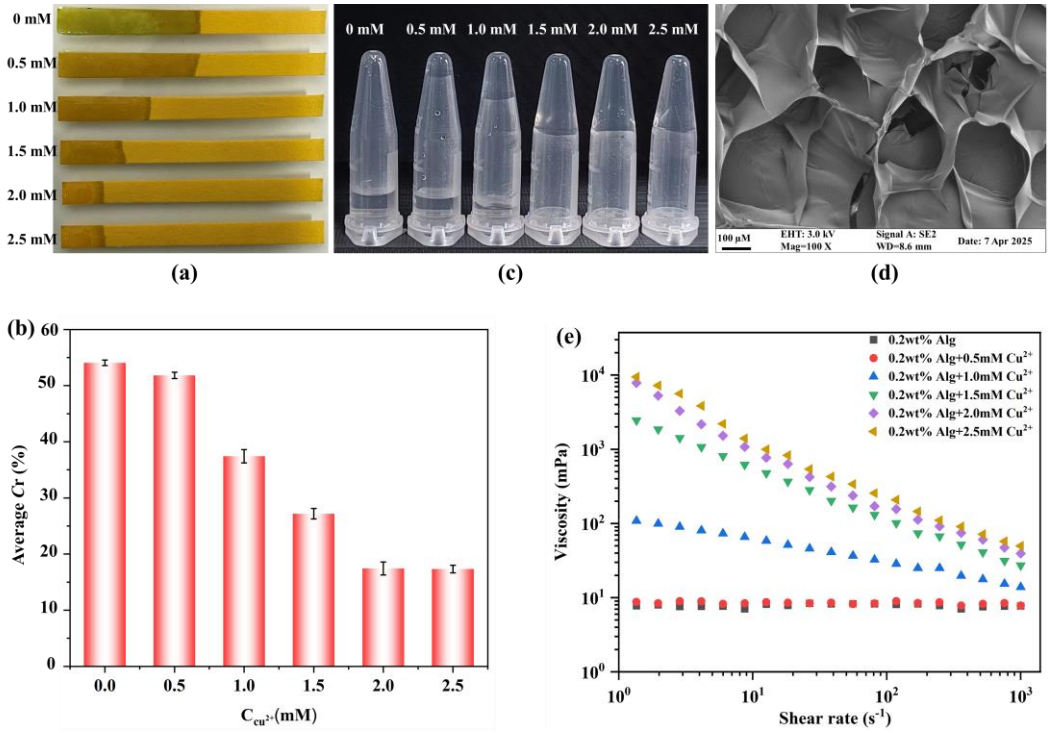

Figure 2. The optimization of the Cu^{2+} concentration for Cu-Alg hydrogel synthesis. (**a**) A photograph and (**b**) the *Cr* values of the flow distance of the Cu-Alg hydrogel on pH papers at different Cu^{2+} concentrations. (**c**) A photograph of the Cu-Alg hydrogel formation in vials at various Cu^{2+} levels. (**d**) An SEM image and (**e**) viscosity against the shear rate of the Cu-Alg hydrogel.

Furthermore, Figure 2c depicts the formation of the Cu-Alg hydrogel at different Cu^{2+} concentrations. The stable Cu-Alg hydrogel is formed at Cu^{2+} concentrations of 2 mM and above. Figure 2e demonstrates the rheological behavior of the Cu-Alg hydrogels. The mixture's viscosity increases with an increasing Cu^{2+} concentration, and when this concentration reaches 2 mM or higher, the viscosity of the resulting hydrogel remains relatively stable. As the Cu^{2+} concentration rises, the three-dimensional network structure of the hydrogel becomes denser, enhancing its ability to capture water molecules. This increase in the Cu-Alg hydrogel's viscosity results in a lower *Cr* value on the pH paper. Based on these findings, we choose a Cu^{2+} concentration of 2 mM to prepare a Cu-Alg hydrogel for further experiments, which is sufficient to restrict the water flow on the pH paper entirely.

3.2. Feasibility of EIDP Biosensor for OP Detection

The feasibility of the EIDP biosensor for OP detection was assessed under various experimental conditions. The Cu-Alg hydrogel restricts water flow on pH paper, resulting in a low Cr value (Figure 3). When a mixture of Cu-Alg hydrogel, AChE, and ATCh was applied, water flow was observed on the pH paper, increasing the Cr value. This increase is due to the formation of thiocholine, which results from AChE hydrolyzing ATCh and has a strong affinity for copper. The interaction between the Cu in the Cu-Alg hydrogel and thiocholine disrupts the three-dimensional structure of the hydrogel, causing a gel–sol transition that allows trapped water to flow onto the pH paper.

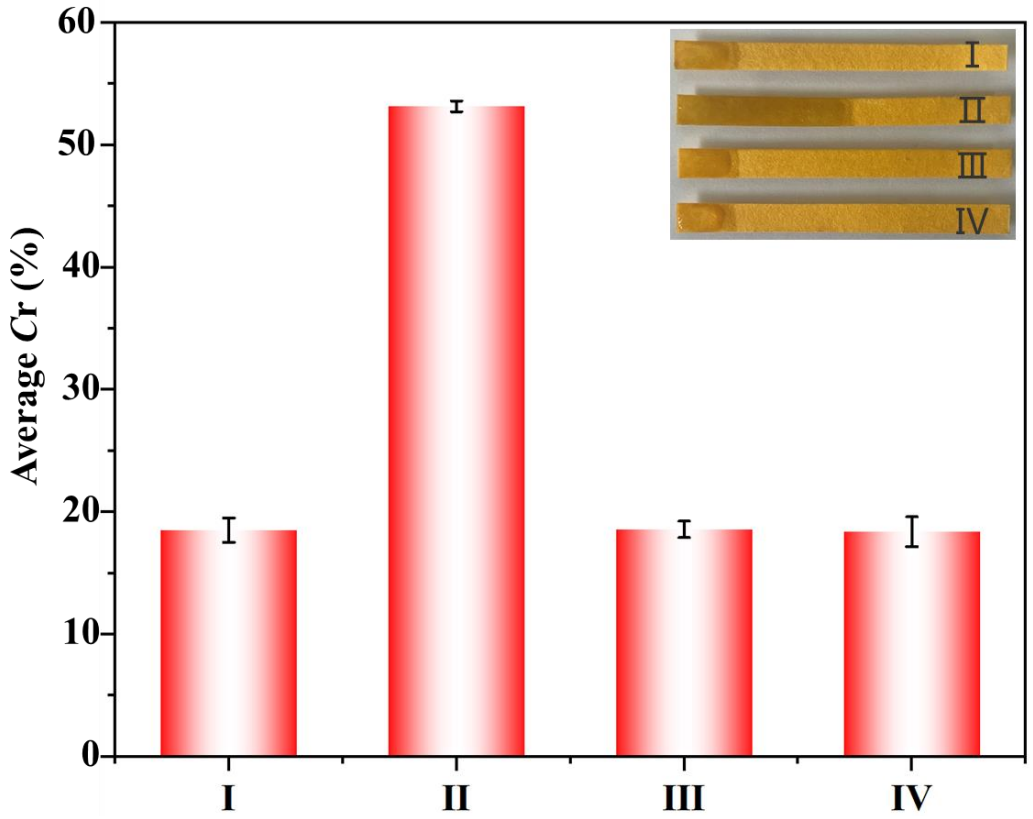

Figure 3. The feasibility of the EIDP biosensor. Cr values from the corresponding flow distance (inset image) under different experimental conditions: (**I**) Cu-Alg, (**II**) Cu-Alg + AChE + ATCh, (**III**) Cu-Alg + ATCH + AChE + OPS, and (**IV**) Cu-Alg + AChE.

Conversely, when OPs were introduced to AChE and subsequently incubated with ATCh and the Cu-Alg hydrogel, there was no water flow on the pH paper, resulting in a low Cr value. This phenomenon occurred because OPs inhibit AChE's activity, preventing it from hydrolyzing ATCH and producing thiocholine. As a result, the three-dimensional structure of the Cu-Alg hydrogel remains intact, and the trapped water cannot escape onto the pH paper. Similarly, utilizing the Cu-Alg hydrogel with AChE alone also resulted in no water flow and a low Cr value. These findings indicate that by employing an optimized ratio of Cu-Alg hydrogel, ATCh, and AChE with varying concentrations of OPs, it is possible to detect OPs in a solution by assessing the water flow distance on pH paper. The ability of OPs to inhibit AChE activity effectively prevents the gel–sol transition, making this detection method viable.

3.3. The Optimization of the Experimental Parameters

Various experimental parameters were analyzed, including the concentrations of AChE and ATCh and the incubation times of AChE with ATCh and OPs. The Cu-Alg

hydrogel, 3 mM ATCh, and varying AChE concentrations (0.02–0.06 U/mL) were incubated and applied to pH paper. The flow distance and the corresponding *Cr* value increased with higher AChE concentrations, peaking at 0.05 U/mL (Figure 4a). Therefore, this concentration of AChE was selected for further experimentation.

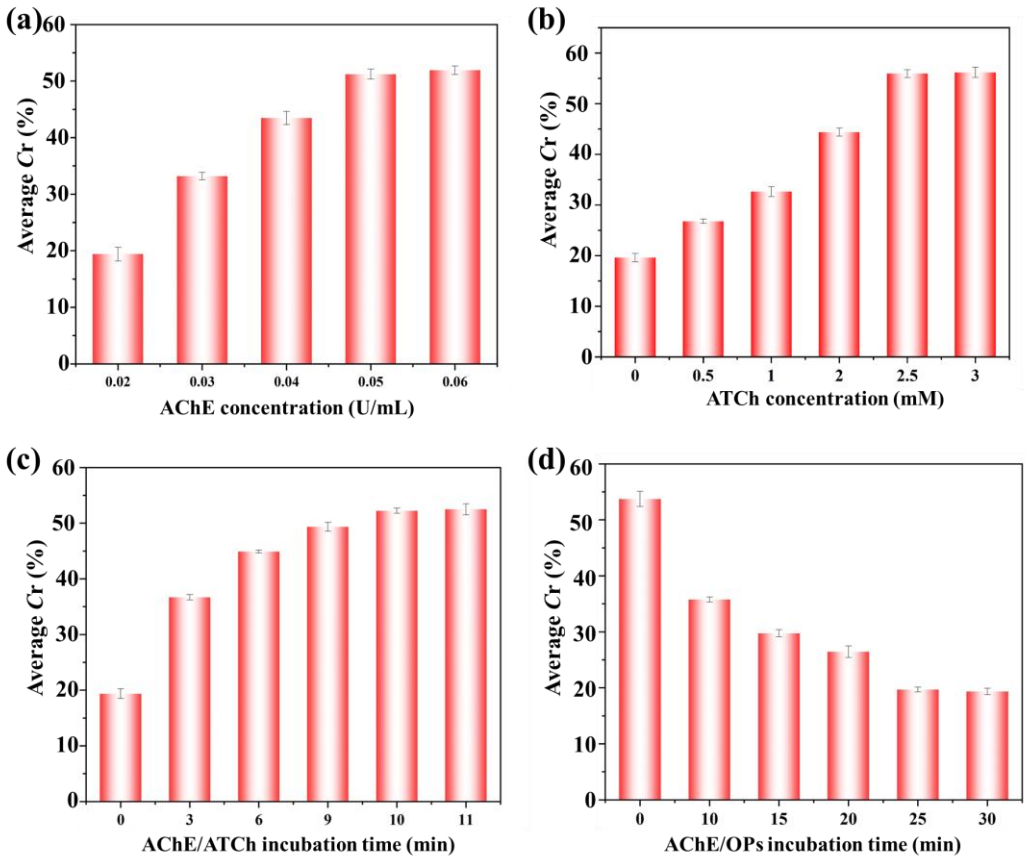

Figure 4. Optimization of experimental parameters. Cr values at different concentrations of (**a**) AChE and (**b**) ATCh when incubated with Cu-Alg. Cr values at various incubation times of (**c**) AChE with ATCh and (**d**) AChE with OPs.

Subsequently, the concentration of AChE's substrate, ATCh, was optimized. Various ATCh concentrations (ranging from 0 to 3 mM) were incubated with the Cu-Alg hydrogel and AChE (0.05 U/mL). At 0.5 mM of ATCh, the formation of thiocholine was insufficient for interaction with the Cu-hydrogel, resulting in only a minor increase in flow distance (Figure 4b). However, as the ATCh concentration increased, the flow distance correspondingly increased, reaching a maximum at an ATCh concentration of 2.5 mM, which stabilized with further increases. Hence, 2.5 mM of ATCh was chosen for further experiments.

The incubation time for the AChE-catalyzed hydrolysis of ATCh was examined. At the onset of the reaction (0 min), all water was confined within the hydrogel, and no water flow on the pH paper, indicated by a low *Cr* value, was observed (Figure 4c). As the incubation time increased, the hydrolysis of ATCh by AChE also escalated, resulting in a higher production of thiocholine. This thiocholine interacted with more Cu^{2+} ions, which loosened the hydrogel's three-dimensional network, allowing water to flow onto the pH paper. Consequently, the *Cr* value increased with longer incubation, peaking at 10 min. Therefore, a 10 min incubation time was used for later experiments.

OPs act as inhibitors of AChE activity, ultimately hindering the hydrolysis of ATCh and the transition from gel to sol. Thus, the optimal incubation time for AChE in the presence of OPs was determined. The AChE was incubated with 100 ng/mL of OPs at various intervals (Figure 4d). Maximum inhibition was observed after 25 min; at this stage,

AChE could not hydrolyze ATCh, resulting in limited water flow on the pH paper. As a result, a low Cr value was recorded at an incubation time of 25 min and beyond. Hence, the optimal incubation period for AChE with OPs was 25 min for all subsequent experiments.

3.4. Sensitivity and Selectivity of OP Detection

The sensitivity of the EIDP biosensor was evaluated at various OP concentrations. Figure 5a shows that the maximum flow distance on the pH paper was observed at OP concentrations of ≤18 ng/mL. As the concentration of OPs increased, the flow distance correspondingly decreased (Figure 5b). A linear relationship exists between OP concentrations and the resulting *C*r values. This indicates that the sensing platform operates within a linear range of 18 to 105 ng/mL, with a correlation coefficient (R^2) of 0.987 (Figure 5b inset). Therefore, the EIDP biosensor offers a simple, portable solution for quantitatively analyzing OPs.

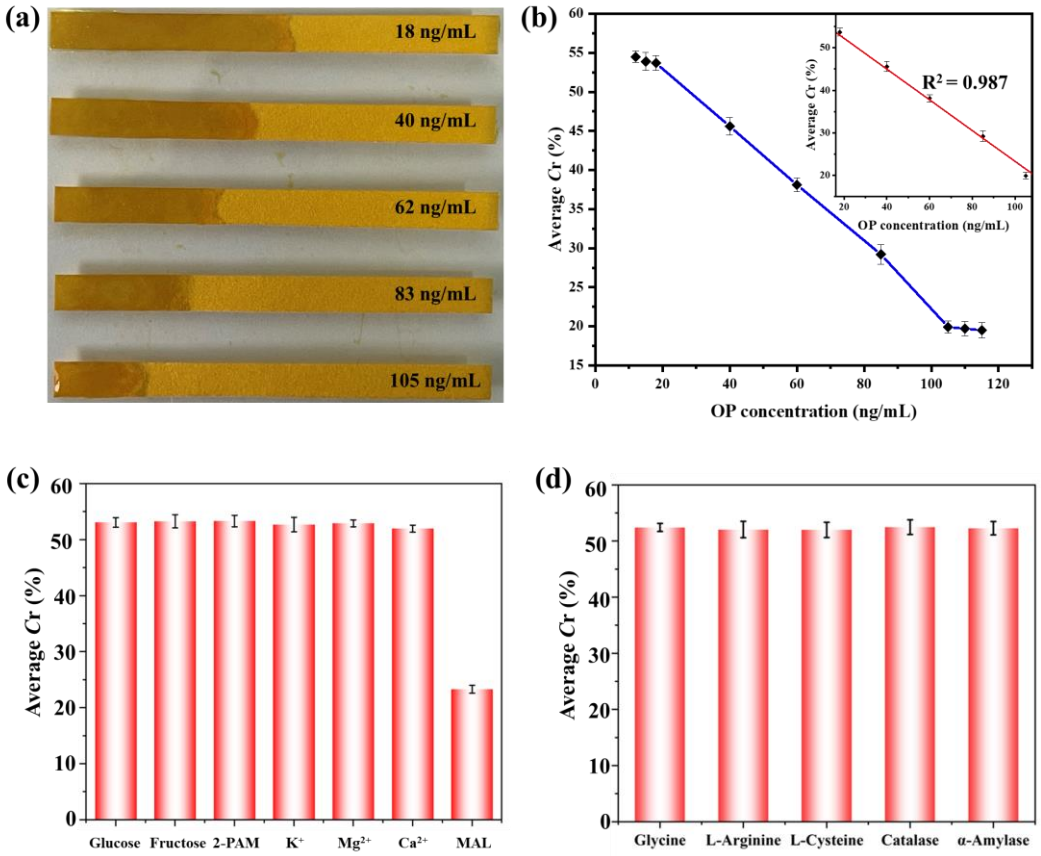

Figure 5. Sensitivity and selectivity of EIDP biosensor. (**a**) Photograph of water flow distance at different OP concentrations. (**b**) Plot of *C*r values as function of OP concentrations; inset figure shows linear range of EIDP biosensor. (**c**,**d**) *C*r values of EIDP biosensor when tested for different potential interfering molecules.

The selectivity of the EIDP biosensor for OPs was evaluated in response to various analytes, including glucose, fructose, 2-PAM, K^+, Mg^{2+}, and Ca^{2+} (Figure 5c), as well as protein and amino acids, such as glycine, L-arginine, L-cysteine, catalase, and α-amylase (Figure 5d). High *C*r values were recorded for all analytes; however, the presence of OPs restricted water flow, leading to a low *C*r value. This observation suggests that the EIDP biosensor exhibits high selectivity in detecting OPs.

3.5. OPs Detection in Pumpkin and Rice Samples

The EIDP biosensor was evaluated to detect OPs in pumpkin and rice samples. Samples were spiked with OP concentrations of 20, 50, and 100 ng/mL, and the amounts of OPs were subsequently analyzed. The results, comparing measured amounts to the spiked concentrations, are displayed in Table 1. In pumpkin and rice samples, the recovery of OPs at the three concentrations ranged from 93% to 103%, with a relative standard deviation of 5.6% to 9.4% (n = 5). These findings indicate that the EIDP biosensor can efficiently analyze OPs in real food samples.

Table 1. Detection of OPs in food samples using EIDP biosensor.

Sample	Spiked OPs (ng/mL)	Measured (ng/mL)	Recovery (%)	RSD (%), n = 5
Pumpkin	20	18.71	93.6	7.6
	50	47.53	95.1	8.8
	100	102.55	102.6	5.6
Rice	20	18.12	90.6	6.5
	50	46.53	93.1	9.4
	100	101.34	101.3	6.1

4. Discussion

We developed an EIDP biosensor platform for the rapid and visual detection of OPs in food samples. This biosensor provides a simple, portable, and cost-effective alternative to traditional analytical methods, effectively addressing the growing demand for on-site monitoring of OPs in food and environmental matrices. The successful application of the biosensor to actual food samples underscores its potential to enhance food safety and safeguard public health.

The EIDP biosensor's high sensitivity is primarily due to the effective inhibition of AChE by OPs, which results in a marked reduction in water flow distance. The Cu-Alg hydrogel significantly enhances this sensitivity because of its responsiveness to the AChE-catalyzed hydrolysis of ATCh. Even a minimal amount of active AChE can facilitate water movement from the Cu-Alg hydrogel onto the pH paper, allowing for the quantitative detection of OPs by measuring the resulting water flow distance.

While GC-MS and HPLC provide high sensitivity and accuracy, their dependence on costly instrumentation and training personnel requirements limits their applicability in resource-constrained environments. In contrast, The EIDP biosensor employs distance-based measurements, offering a more quantitative and objective readout than other paper-based colorimetric assays. This approach significantly minimizes the subjectivity often linked to visual color interpretation. Consequently, the EIDP biosensor stands out as a cost-effective and user-friendly alternative for the on-site detection of OPs.

The detection of OPs in pumpkin and rice samples, with recoveries ranging from 93% to 103%, demonstrates the accuracy and reliability of the EIDP biosensor for real-world applications. These findings suggest that the biosensor can mitigate matrix interferences commonly encountered in complex food samples. A straightforward extraction procedure was implemented before analysis to minimize potential matrix effects. This pretreatment step effectively removed interfering substances, enhancing the overall accuracy of the biosensor.

While the EIDP biosensor offers several advantages, it also has some limitations. The current biosensor is limited to detecting a specific range of OPs. Future research should focus on expanding the range of detectable OPs and improving the long-term stability of the biosensor.

5. Conclusions

An EIDP biosensor was developed to detect OPs. This biosensor functions by monitoring the inhibition of AChE activity on ATCh in the presence of OPs, which influences the flow of trapped water within a Cu-Alg hydrogel on pH paper. The concentration of OPs is assessed by measuring the reduction in water flow distance on the pH paper. In the absence of OPs, a substantial flow distance is observed; however, water flow is fully restricted at an OP concentration of 105 ng/mL. The EIDP biosensor exhibits high selectivity for OPs when tested alongside other analytes such as glucose, fructose, K^+, Mg^{2+}, and Ca^{2+}. Moreover, it enables accurate analysis of OPs in pumpkin and rice samples. This biosensor offers a straightforward, instrument-free, efficient, and label-free method for visually detecting OPs in food products.

Author Contributions: Conceptualization, Y.L., Q.H. and M.K.; methodology, Y.L. and L.D.; software, Y.L.; validation, Y.L., Q.H. and M.K.; formal analysis, Y.L., L.D. and J.C.; investigation, Y.L. and L.D.; resources, Q.H. and M.K.; data curation, Y.L., Q.H. and M.K.; writing—original draft preparation, Y.L. and M.K.; writing—review and editing, Q.H., J.C. and M.K.; visualization, Y.L.; supervision, Q.H. and M.K.; project administration, Q.H. and M.K.; funding acquisition, Q.H. and M.K. All authors have read and agreed to the published version of the manuscript.

Funding: We acknowledge the financial support from the Natural Science Foundation of Shandong Province (No. ZR2022MB147 and ZR2021QH106) and the Science, Education, and Industry Integration Pilot Project for Talent Research at Qilu University of Technology (Shandong Academy of Sciences) (2024RCKY033).

Institutional Review Board Statement: Not applicable.

Informed Consent Statement: Not applicable.

Data Availability Statement: The original contributions presented in this study are included in the article. Further inquiries can be directed to the corresponding authors.

Conflicts of Interest: The authors declare no conflicts of interest. The funders had no role in the study's design, data collection, analysis, or interpretation; in the writing of the manuscript writing; or in the decision to publish the results.

Abbreviations

The following abbreviations are used in this manuscript:

EIDP	Enzyme inhibition-mediated distance-based paper
OPs	Organophosphate pesticides
ATCh	Acetylthiocholine iodide
AChE	Acetylcholinesterase
Cu-Alg	Copper alginate
2-PAM	2-Pyridinealdoxime methochlorid

References

1. Songa, E.A.; Okonkwo, J.O. Recent approaches to improving selectivity and sensitivity of enzyme-based biosensors for organophosphorus pesticides: A review. *Talanta* **2016**, *155*, 289–304. [CrossRef] [PubMed]
2. Ding, T.-T.; Zhang, Y.-H.; Zhu, Y.; Du, S.-L.; Zhang, J.; Cao, Y.; Wang, Y.-Z.; Wang, G.-T.; He, L.-S. Deriving water quality criteria for China for the organophosphorus pesticides dichlorvos and malathion. *Environ. Sci. Pollut. Res.* **2019**, *26*, 34622–34632. [CrossRef] [PubMed]
3. Čadež, T.; Kolić, D.; Šinko, G.; Kovarik, Z. Assessment of four organophosphorus pesticides as inhibitors of human acetylcholinesterase and butyrylcholinesterase. *Sci. Rep.* **2021**, *11*, 21486. [CrossRef] [PubMed]
4. Zoofaghari, S.; Maghami-Mehr, A.; Abdolrazaghnejad, A. Organophosphate Poisoning: Review of Prognosis and Management. *Adv. Biomed. Res.* **2024**, *13*, 82. [CrossRef]

5. Shekhar, C.; Khosya, R.; Thakur, K.; Mahajan, D.; Kumar, R.; Kumar, S.; Sharma, A.K. A systematic review of pesticide exposure, associated risks, and long-term human health impacts. *Toxicol. Rep.* **2024**, *13*, 101840. [CrossRef]
6. Kumaran, A.; Vashishth, R.; Singh, S.; U, S.; James, A.; Velayudhaperumal Chellam, P. Biosensors for detection of organophosphate pesticides: Current technologies and future directives. *Microchem. J.* **2022**, *178*, 107420. [CrossRef]
7. Zhu, B.; Xu, X.; Luo, J.; Jin, S.; Chen, W.; Liu, Z.; Tian, C. Simultaneous determination of 131 pesticides in tea by on-line GPC-GC–MS/MS using graphitized multi-walled carbon nanotubes as dispersive solid phase extraction sorbent. *Food Chem.* **2019**, *276*, 202–208. [CrossRef]
8. Erhard, M.H.; Schmidt, P.; Kühlmann, R.; Lösch, U. Development of an ELISA for detection of an organophosphorus compound using monoclonal antibodies. *Arch. Toxicol.* **1989**, *63*, 462–468. [CrossRef]
9. Ioerger, B.P.; Smith, J.S. Multiresidue method for the extraction and detection of organophosphate pesticides and their primary and secondary metabolites from beef tissue using HPLC. *J. Agric. Food Chem.* **1993**, *41*, 303–307. [CrossRef]
10. Qiu, L.; Lv, P.; Zhao, C.; Feng, X.; Fang, G.; Liu, J.; Wang, S. Electrochemical detection of organophosphorus pesticides based on amino acids conjugated nanoenzyme modified electrodes. *Sens. Actuators B Chem.* **2019**, *286*, 386–393. [CrossRef]
11. Loguercio, L.F.; Griep, J.; Demingos, P.G.; Morawski, R.; Brolo, A.G.; Andrade, G.F.S.; Santos, J.F.L. Enhanced enzymatic electrochemical detection of an organophosphate Pesticide: Achieving Wide linearity and femtomolar detection via gold nanoparticles growth within polypyrrole films. *Talanta* **2025**, *281*, 126714. [CrossRef] [PubMed]
12. Hassani, S.; Momtaz, S.; Vakhshiteh, F.; Maghsoudi, A.S.; Ganjali, M.R.; Norouzi, P.; Abdollahi, M. Biosensors and their applications in detection of organophosphorus pesticides in the environment. *Arch. Toxicol.* **2017**, *91*, 109–130. [CrossRef] [PubMed]
13. Kaur, J.; Singh, P.K. Enzyme-based optical biosensors for organophosphate class of pesticide detection. *Phys. Chem. Chem. Phys.* **2020**, *22*, 15105–15119. [CrossRef] [PubMed]
14. Yang, C.-L.; Yu, L.-H.; Pang, Y.-H.; Shen, X.-F. A ratiometric fluorescence sensor for detection of organophosphorus pesticides based on enzyme-regulated multifunctional Fe-based metal-organic framework. *Talanta* **2024**, *278*, 126516. [CrossRef]
15. Yousefi, R.; Asgari, S.; Banitalebi Dehkordi, A.; Mohammadi Ziarani, G.; Badiei, A.; Mohajer, F.; Varma, R.S.; Iravani, S. MOF-based composites as photoluminescence sensing platforms for pesticides: Applications and mechanisms. *Environ. Res.* **2023**, *226*, 115664. [CrossRef]
16. Jing, W.; Shi, Q.; Qiang, S.; Wang, Y.; Li, Y.; Zhao, T.; Li, Y.; Liu, D.; Liu, Y.; Liu, F. Dual-mode colorimetric and chemiluminescence aptasensor for organophosphorus pesticides detection using aptamer-regulated peroxidase-like activity of TA-Cu. *Talanta* **2025**, *285*, 127410. [CrossRef]
17. Yu, H.; Wang, M.; Cao, J.; She, Y.; Zhu, Y.; Ye, J.; Abd El-Aty, A.M.; Hacımüftüoğlu, A.; Wang, J.; Lao, S. Dual-mode detection of organophosphate pesticides in pear and Chinese cabbage based on fluorescence and AuNPs colorimetric assays. *Food Chem.* **2021**, *364*, 130326. [CrossRef]
18. Meng, X.; Wei, J.; Ren, X.; Ren, J.; Tang, F. A simple and sensitive fluorescence biosensor for detection of organophosphorus pesticides using H2O2-sensitive quantum dots/bi-enzyme. *Biosens. Bioelectron.* **2013**, *47*, 402–407. [CrossRef]
19. Bhattu, M.; Verma, M.; Kathuria, D. Recent advancements in the detection of organophosphate pesticides: A review. *Anal. Methods* **2021**, *13*, 4390–4428. [CrossRef]
20. Chaudhari, P.; Chau, L.-K.; Ngo, L.T.; Chang, T.-C.; Chen, Y.-L.; Huang, K.-T. Competitive Assay for the Ultrasensitive Detection of Organophosphate Pesticides Based on a Fiber-Optic Particle Plasmon Resonance Biosensor and an Acetylcholinesterase Binding Peptide. *Anal. Chem.* **2023**, *95*, 14600–14607. [CrossRef]
21. Khan, M.; Zhao, B.; Wu, W.; Zhao, M.; Bi, Y.; Hu, Q. Distance-based microfluidic assays for instrument-free visual point-of-care testing. *TrAC Trends Anal. Chem.* **2023**, *162*, 117029. [CrossRef]
22. Jiang, C.; Wang, F.; Zhang, K.; Min, T.; Chen, D.; Wen, Y. Distance-Based Biosensor for Ultrasensitive Detection of Uracil-DNA Glycosylase Using Membrane Filtration of DNA Hydrogel. *ACS Sens.* **2021**, *6*, 2395–2402. [CrossRef] [PubMed]
23. Xiao, Y.; Wang, X.; Yin, Y.; Yin, F.; Li, J.; Hou, Z.; Khan, M.; Zhao, R.; Wu, W.; Hu, Q. Distance-based lateral flow biosensor for the quantitative detection of bacterial endotoxin. *Chin. Chem. Lett.* **2024**, *35*, 109718. [CrossRef]
24. Han, C.; Yuan, X.; Shen, Z.; Xiao, Y.; Wang, X.; Khan, M.; Liu, S.; Li, W.; Hu, Q.; Wu, W. A paper-based lateral flow sensor for the detection of thrombin and its inhibitors. *Anal. Chim. Acta* **2022**, *1205*, 339756. [CrossRef] [PubMed]
25. Chen, Y.; Chu, W.; Liu, W.; Guo, X. Distance-based carcinoembryonic antigen assay on microfluidic paper immunodevice. *Sens. Actuators B Chem.* **2018**, *260*, 452–459. [CrossRef]
26. Tai, W.; Yin, F.; Bi, Y.; Lin, J.-M.; Zhang, Q.; Wei, Y.; Hu, Q.; Yu, L. Paper-based sensors for visual detection of alkaline phosphatase and alpha-fetoprotein via the distance readout. *Sens. Actuators B Chem.* **2023**, *384*, 133666. [CrossRef]
27. Wang, H.; Liu, Z.; Xiao, J.; Li, C.; Wang, J.; Xiao, X.; Huang, H.; Shrestha, B.; Tang, L.; Deng, K.; et al. Visual Quantitative Detection of Glutathione and Cholesterol in Human Blood Based on the Thiol–Ene Click Reaction-Triggered Wettability Change of the Interface. *Anal. Chem.* **2021**, *93*, 7292–7299. [CrossRef]

28. Ho, M.; Sathishkumar, N.; Sklavounos, A.A.; Sun, J.; Yang, I.; Nichols, K.P.; Wheeler, A.R. Digital microfluidics with distance-based detection—A new approach for nucleic acid diagnostics. *Lab Chip* **2023**, *24*, 63–73. [CrossRef]
29. Allameh, S.; Rabbani, M. A Distance-Based Microfluidic Paper-Based Biosensor for Glucose Measurements in Tear Range. *Appl. Biochem. Biotechnol.* **2022**, *194*, 2077–2092. [CrossRef]
30. Jiang, C.; Li, Y.; Wang, H.; Chen, D.; Wen, Y. A portable visual capillary sensor based on functional DNA crosslinked hydrogel for point-of-care detection of lead ion. *Sens. Actuators B Chem.* **2020**, *307*, 127625. [CrossRef]

Disclaimer/Publisher's Note: The statements, opinions and data contained in all publications are solely those of the individual author(s) and contributor(s) and not of MDPI and/or the editor(s). MDPI and/or the editor(s) disclaim responsibility for any injury to people or property resulting from any ideas, methods, instructions or products referred to in the content.